

XII International Conference on Computational Plasticity. Fundamentals and Applications
COMPLAS XII
E. Oñate, D.R.J. Owen, D. Peric and B. Suárez (Eds)

MULTI-SCALE ANALYSIS OF TIMBER FRAMED STRUCTURES FILLED WITH EARTH AND STONES

F. VIEUX-CHAMPAGNE*, S. GRANGE*, Y. SIEFFERT*,
L. DAUDEVILLE*

* UJF-Grenoble 1, Grenoble-INP, CNRS UMR 5521, 3SR Lab, Grenoble F-38041, France
e-mail: florent.vieux-champagne@3sr-grenoble.fr, web page: <http://3sr.hmg.inpg.fr/3sr/>

Key words: Timber framed structure, Mutli-scale, Filled, Shear walls, Finite element, Constitutive model, Stones, Earth

Abstract. This paper deals with the seismic analysis of timber framed houses filled by stones and earth mortar using a multi-scale approach going from the cell to the wall and then to the house. At the scale of the elementary cells, experimental results allow fitting the parameters of a new versatile hysteretic law presented herein through the definition of a macro-element. Then, at the scale of wall, the numerical simulations are able to predict its behavior under quasi-static cyclic loading and is compared to experimental results allowing validating the macro-element model.

1 INTRODUCTION

During the earthquake that struck Haiti, on the 12th of January 2010, a great number of concrete block and reinforced concrete buildings were heavily damaged. The destruction or collapse of these buildings had a dramatic impact in terms of human life and huge economical loss for the country. In urban areas as well as in rural ones traditional timber frame buildings did not suffer that much, showing an enhanced structural behaviour and exposing their inhabitants to a limited risk, thanks to their lower seismic vulnerability and cost (see [7]).

These findings raise the issue of the very limited importance given to local architectures by the scientific community and by those responsible for reconstruction, despite the fact that in Haiti as well as in other places, those structures have often shown highly relevant use of technical solutions and available resources, in relation to the constraints and the potential of the context.

Within the framework of the ReparH project, supported by the French National Research Agency (ANR), a scientific collaboration was established between researchers in the field of architecture (CRATERRE-ENSAG) and engineering (3SR - UJF) with the Haitian

organization GADRU, to carry out a technical and methodological reflection to support the development of sustainable reconstruction and vulnerability reduction strategies.



(a) Traditional (SCCF NGO)

(b) Built for a reconstruction project (Misereor NGO)

Figure 1: rural Haitian houses

In this paper an experimental approach performed previously is now compared with traditional timber-frame constructions (see Fig. 1) by means of multi-scale non-linear numerical analysis.

The proposed method includes numerical studies from the connections to the wall elementary cell (square braced by a St Andrew cross, Fig. 4(a)), to the entire wall (Fig. 6(a)) and then to the whole house. More details about this multi-scale approach are given in the references section ([4], [8] and [9]).

This multi-scale approach illustrated in Fig. 2 aims at modelling shear walls or whole buildings with a very limited number of degrees of freedom (about 500 for the whole house) without losing simulation accuracy. This approach allows reducing significantly computational cost and computational efforts for the user to realize the mesh. In addition, the multi-scale approach is really suitable in this study because experimental data are easily obtained at connection and cell levels. It is then possible to reproduce numerically the behavior of cells. From this first analysis at the cell scale, hysteretic behavior of the cell is fitted correctly using a modification of the 1-D law presented herein and in [6] (see Fig. 3) as a macro-element (Fig. 4(d)).

2 PRESENTATION OF THE HYSTERETIC MODEL FOR THE MACRO-ELEMENT

A one dimensional constitutive model in order to build the macro-element is presented in [1] and shown in Fig. 3. This constitutive law allows reproducing elasticity, plastic and residual strains, damage and pinching effect. The branches of the force–displacement model are grouped into two distinct categories and numbered from (0) to (5). A first

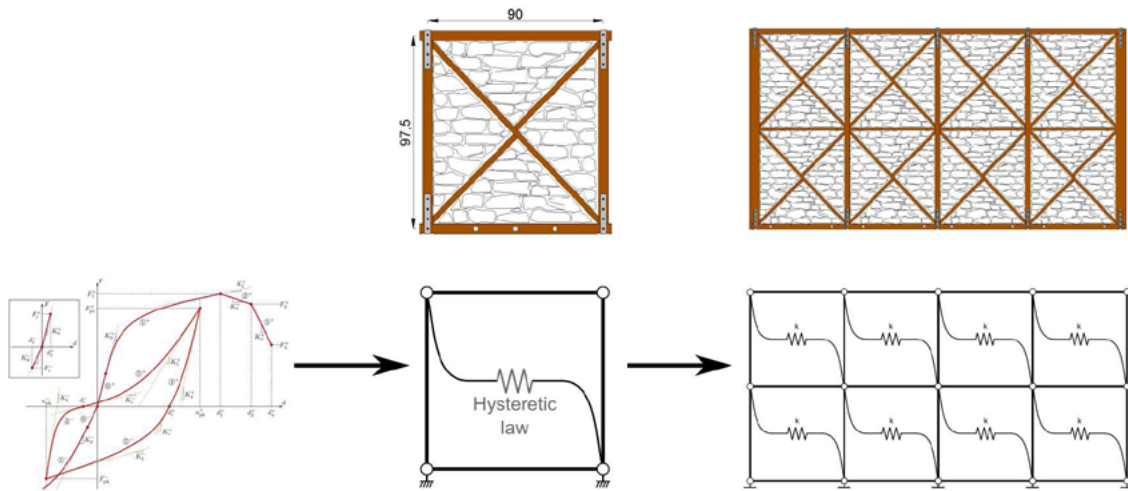


Figure 2: Multi-scale approach

group formed by branches (0) to (3) describes the behaviour under monotonic loading. The initial linear branch (0) ranges from the zero displacement up to the yield displacement d_y . The corresponding elastic stiffness is K_0 . This branch is followed by branch (1), which models the non-linear phenomena in the joint up to the force peak at (d_1, F_1) . After the force peak, branches (2) and (3) model up to the ultimate displacement d_u at force F_u associated to the collapse of the joint. F_u is generally chosen null to ensure a correct continuity of forces and prevent numerical issues. Therefore, 9 parameters describe the force–displacement behaviour under monotonic loading. Branch (1) is defined using a rational quadratic Bézier curve and provides a strict analytical continuity of forces.

A second group of branches describes the hysteresis loops which are typically observed when the joint undergoes a reversed loading. Starting from a previously reached loop peak (u_{pk}, F_{pk}) , branch (4) models the non-linear elastic unloading down to a null force. A residual displacement $d_c \neq 0$ is commonly observed due to prior plastic deformations. The unloading stiffness K_4 is either: a) proportional to the elastic stiffness K_0 of the joint; or b) proportional to the secant stiffness F_{pk}/u_{pk} in order to model a stiffness decrease with displacements of increasing amplitude. Following this unloading, loading in the opposite direction is modelled with branch (5). The stiffness at d_c between branches (4) and (5) is denoted K_c and is used as a tangent for both branches for the sake of continuity. Branch (5) eventually reaches the previous loop peak $(u_{pk}^\bullet, F_{pk}^\bullet)$ in the opposite loading direction. Like the unloading stiffness K_4 , the reloading stiffness K_5 is proportional to the elastic stiffness K_0 or to the secant stiffness F_{pk}/u_{pk} . A second set of 4 control parameters $C_{i=1,\dots,4}$ governs the shape of the hysteresis loops. This allows modelling several mechanical behaviours, in particular, the thickness of the pinching area can be adjusted. Parameters C_1 and C_2 control the unloading stiffness K_4 and reloading stiffness K_5 respectively. Parameter C_3 controls the tangent stiffness K_c at location

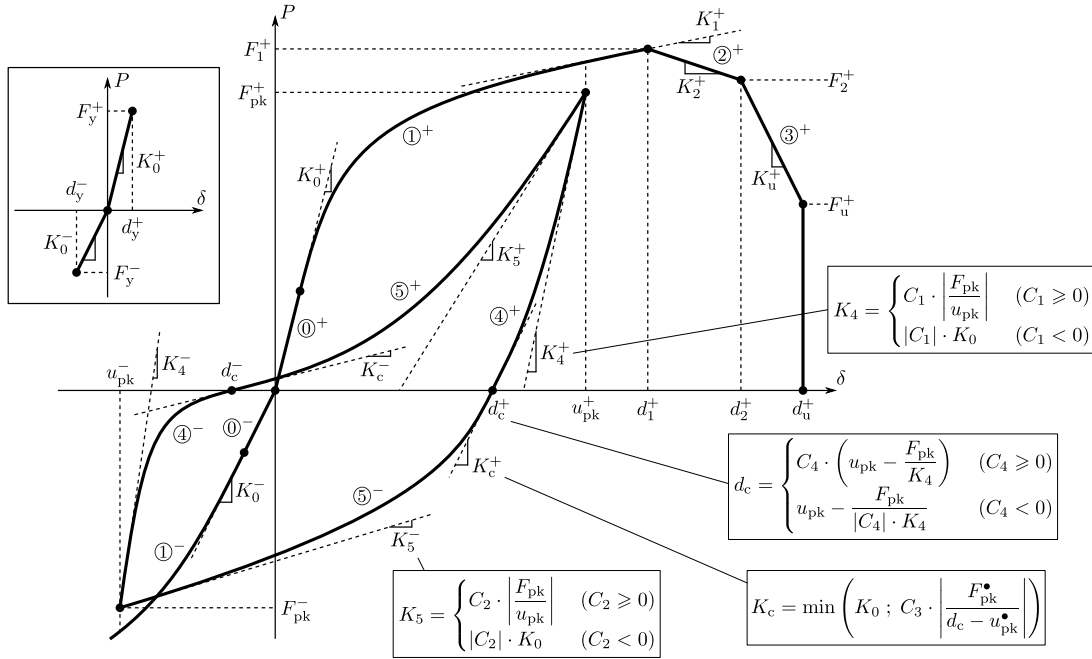


Figure 3: Proposed force–displacement model ([6])

$(d_c, 0)$. Finally, parameter C_4 controls the value of the residual displacement d_c after the non-linear elastic unloading. These 4 control parameters $C_{i=1, \dots, 4}$ depend mainly on the phenomena involved, and therefore on the configuration of the modelled system. They are constant for a given configuration.

Finally, a third set of 3 parameters controls the damage process under cyclic loading of the model. The word *damage* refers here to the decrease of strength under cyclic. It is based on the hypothesis that the hysteresis loops are bound by the backbone curve which models the force–displacement evolution of the joint under monotonic loading. During the first loading, the peak (u_{pk}, F_{pk}) is located on the backbone curve. The damage process defines the evolution of the ratio $(1-D)$ between the “non-damaged load” F_{mono} and the “damaged load” F_{pk} . The scalar damage indicator D ranges from 0 to 1, where $D = 0$ corresponds to a non-damaged mechanical system and $D = 1$ corresponds to a fully collapsed mechanical system. D is increased of ΔD at each change of the force sign ((4) to (5) in Figure 3). To ensure the damage stabilization after a few cycles of constant amplitude as experimentally observed, an upper limit D_∞ for the displacement d_{max} is defined, using a power law (eq 1). A power term $B_r > 1$ ensures that the damage remains moderate before the force peak and becomes heavy after the peak.

$$D_\infty = B_c (d_{max}/d_1)^{B_r} \quad (1)$$

3 CELL'S SCALE - FITTING PARAMETERS

In this part, the elementary cell is described and the macro-element is defined. Then, the calibration of this simplified element is presented with the corresponding parameters of the law.

3.1 Structure and simplified FE model

The elementary cell shown in Fig. 4(a) is made of four wood beams connected together by punched steel strip nailed by $3\text{ mm} \times 70\text{ mm}$ common nails (see Fig. 4(b)). It is braced by wood bars X-crossed and filled with a stone masonry and an earth mortar. It can be noted that X-cross is not symmetric. One of these bar goes from the top to the bottom whereas the second one is split in two parts and linked to the first one at the middle of the cell. More properties of this structure are given in the fourth part.

The cell is designed to be as close as possible of the wall's part represented in Fig. 6(a). Nevertheless the boundary conditions are not exactly the same due to practices issues. The upper and the bottom part of the cell, made with type 1-joint (see Fig. 4(b)), match with the same parts of the wall. Therefore, the middle part of the wall, made with type 2-joint (see Fig. 4(c)), is not included in the elementary cell.

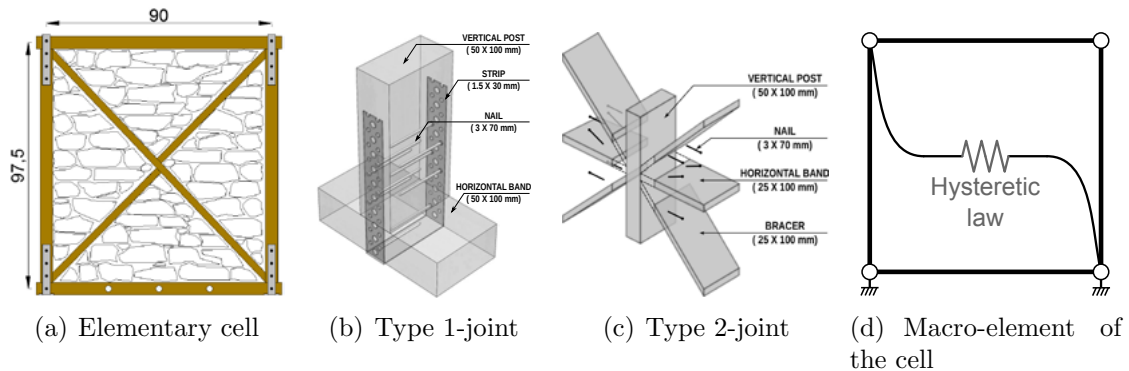
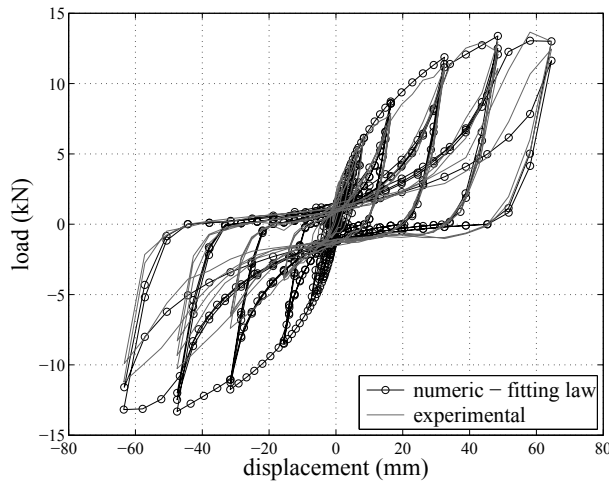


Figure 4: Cell – Experimental and modelling

The experimental campaign on elementary cell involved two reversed cyclics and one monotonic quasi-static tests per configuration. The influence of the kind and the presence of filling and bracing were tested but these experiments are not presented herein. The loading was applied on top beam of the structure.

The macro-element, simplified FE model, shown in Fig. 4(d)) is composed of 4 bars where the right upper node is linked with left bottom node with the 1D non linear constitutive law presented above. This representation allow concentrating all the non-linearities of the cell in one global element. It ensures the hypothesis of a parallelogram-like deformation of the cell, therefore modelling only the shearing behaviour (*i.e.* in and out-of-plane bending and overturning effects are not taken into account). This hypothesis is based on previous studies [5] and experimental observations.



K_0	1.7e6	N/m	C_1	-1.0
d_y	5.0e-4	m	C_2	-1.0
d_1	3.8e-2	m	C_3	1.0e-1
F_1	1.3e4	N	C_4	8.0e-1
K_1	1.5e5	N/m	B_c	1.2e-1
d_2	6.0e-2	m	B_r	2.0
F_2	1.0e4	N	η	5.0e-1
d_u	8.0e-2	m		
F_u	7.5e4	N		

Figure 5: Calibration of the model on an experimental test and the model’s parameters

3.2 Calibration of the parameters at the cell’s level

The law is implemented in AGALab, a finite element code developed in Matlab[®] by 3SR team

The results of the tests performed on the cells are used to calibrate the constitutive model. The calibration consists in reproducing one particular test as displayed in Fig. 5. Normally, it is obtained by calculating the backbone curve parameters from monotonic test(s) and by calibrating the pinching and damage parameters from cyclic test(s). Herein, only one cyclic test is used to fit the parameters because the difference between the backbone curve and the envelop curve of a cycle test is very low and because the repeatability of the cycle tests is good.

The coefficients are the same in both positive and negative directions which lead to a symmetric numerical curve. Therefore only the positive parameters used to the calibration are given in the table of the figure 5.

Nevertheless, it can be noted an asymmetry of the experimental curve which can be explained by the difference between the continuous plank and the perpendicular two parts of the X-cross. When the cell’s diagonal made of two bars is under a compressive strength, the stiffness is lower as shown in the graph of Fig. 5 (negative displacement). That’s why the calibration has been done only on the positive side of the experimental curve.

4 WALL’S SCALE - PREDICTION OF ITS GLOBAL BEHAVIOR

In this part, the structure of the wall is described. Then, a mesh of the wall using an association of the macro-element is presented. Finally a prediction of the wall’s behaviour under quasi-static loading given by the model is compared with an experimental test.

4.1 Structure and modelling

The structure of the wall is displayed on Fig. 6(a). It is 1.975 meter high and 3.75 meters wide. It is composed of two $10\text{ cm} \times 10\text{ cm}$ posts at both extremities and three $5\text{ cm} \times 10\text{ cm}$ in the center. They are linked with a bottom and an upper $5\text{ cm} \times 10\text{ cm}$ wood beam by the mean of punched steel strip FP30/1,5/50 from Simpson Strong-Tie®, 30 mm wide and 1,5 mm thick. 3 mm \times 70 mm common steel wire nails are used (see [2]) to fixed the strip. Timber strength class is C18 with a density $\rho_{mean} = 380\text{ kg/m}^3$ according to the European standard EN 338 (see [3]).

The experimental campaign has been realised at the CNR-Ivalsa in Trento, Italy, where three filled wall were tested : two cycle tests and one monotonic.

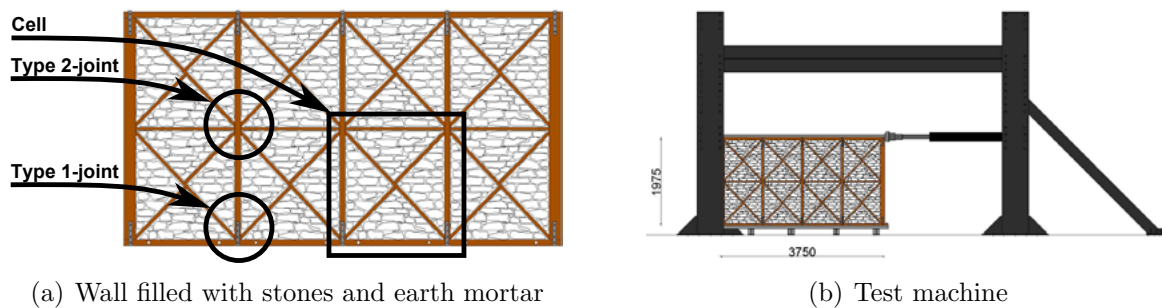


Figure 6: A wall and the test machine

The mesh of the wall using the association of the macro-elements is described in Fig. 7. Kinematic links in both directions of the different nodes at the interface of the macro-elements are also presented.

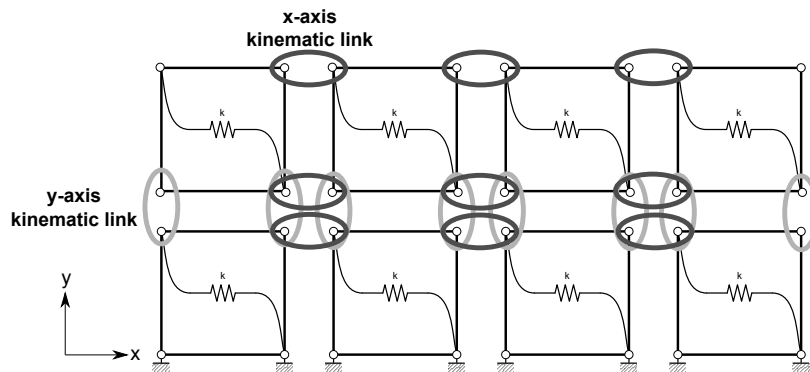


Figure 7: Mesh of the wall using an association of macro-element

4.2 Comparison between numerical and experimental results

The prediction of the wall's behavior is provided in Fig. 8. Regarding the resisting force prediction, the model shows good results with only 11% of error. The difference can be explained by the fact that the type 2-joints energy dissipation is not taken into account.

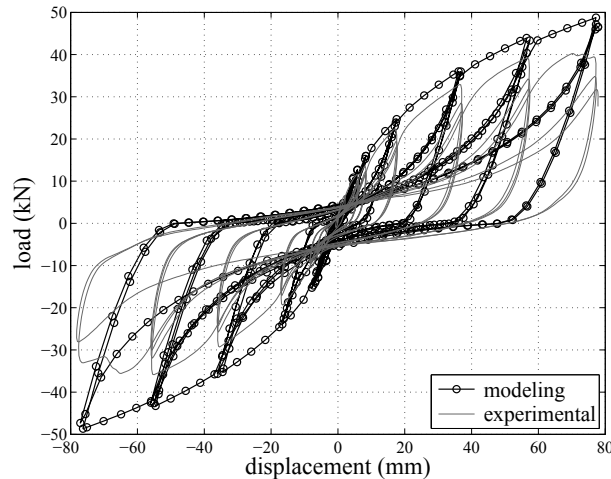


Figure 8: Prediction of the wall's behavior – Experimental versus numerical results

Then, it can be noticed that the wall model cannot predict softening due to damage effect appearing for top displacements of about 40 *mm*. In the numerical results, the softening appears for top displacements of about 80 *mm* when using the parameters fitted at the cell's level.

Ongoing research aims at adding supplementary features to be able to take into account the type 2-connection and the damage effect.

The computation effort to implement the model and the computational cost are low. Therefore in comparison with the simplicity of the model, the prediction is satisfactory and validates this simplified approach.

5 CONCLUSIONS

This paper presents a simplified finite element analysis study about traditional wood structure filled with stones and an earth mortar. The first part describes the constitutive law allowing to accurately reproduce the hysteretic behavior, damage and pinching effect. Then, application of this law is illustrated in a multi-scale study by reproducing the experimental behavior of a cell under quasi-static loading in order to build a macro-element. The third part presents the prediction of the experimental wall's behavior by mean of a simplified FE model composed of the macro-element's association. This multi-scale approach is very simple and allow to predict the behavior of timber frame wall filled

with stones and earth mortar.

Ongoing research aims to model the the whole house by using only 500 degree of freedoms using the same macro-element as shown on Fig.9. An experimental test on an uni-axial shaking table at the house's scale was performed at the FCBA, Bordeaux in April 2013 and will allow to validate at the third scale to validate the multi-scale approach presented herein.

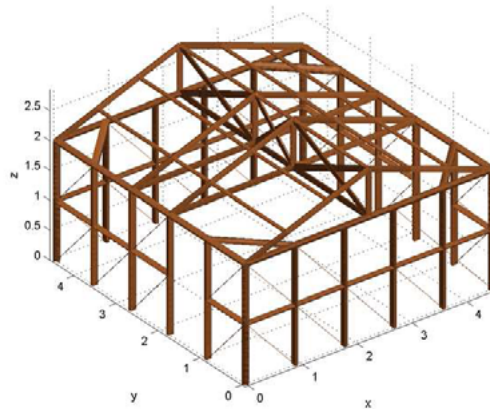


Figure 9: Modelling of a whole house with the macro-element

6 ACKNOWLEDGMENT

The french agency ANR is gratefully acknowledged for funding this research ANR-10-HAIT-003.

Philippe Garnier is also acknowledged for the management of this project.

References

- [1] C. Boudaud, J. Baroth, S. Hameury, and L. Daudeville. Multi-scale modelling of timber-frame structures under seismic loading. *XII International Conference on Computational Plasticity*, 2013.
- [2] EN 10230-1. *Steel Wire Nails - Part 1: Loose Nails For General Applications*, 2000.
- [3] EN 338. *Structural timber - Strength classes*, 2003.
- [4] B. Folz and A. Filiatrault. Cyclic analysis of wood shear walls. *Journal of Structural Engineering*, 127(4), pp 433-441, 2001.
- [5] A.K. Gupta and G.P. Kuo. Behavior wood-framed shear walls. *Journal of Structural Engineering*, 111(8), 1722-1733, 1985.
- [6] J. Humbert. *Characterization of the behavior of timber structures with metal fasteners undergoing seismic loadings*. PhD thesis, Grenoble University, 2010.

- [7] R. Langenbach. "crosswalls" instead of shearwalls. *5th National Conference on Earthquake Engineering*, 2003.
- [8] N. Richard. *Approche multi-échelles pour la modélisation de structures en bois sous sollicitations sismiques*. PhD thesis, Ecole Normale Supérieure de Cachan, Laboratoire de Mécanique et Technologie, 2001.
- [9] J. Xu and J.D. Dolan. Development of a wood-frame shear wall model in abaqus. *Journal of structural engineering*, 135(8), 977-984, 2009.